

Improved sensor sensitivity and light-matter interaction through linear width grading

B. Mohapatra¹, D. Dash², D. Gupta¹

¹Department of Electronics & Communication Engineering, Greater Noida Institute of Technology (Engineering Institute), Uttar Pradesh, India-201310

²Department of Electrical & Electronics Engineering, Galgotias College of Engineering & Technology, Uttar Pradesh, India-201310

*Corresponding author e-mail: dash.diptimayee@gmail.com

Abstract. This paper introduces a proposal for a linearly width graded photonic crystal featuring a central defect layer specifically designed for sensing applications. The design entails incorporating alternating layers of a dielectric material onto a glass substrate. Introducing intentional porosity within each layer facilitates analyte infiltration and enhances sensitivity. Comprehensive analysis is conducted to optimize the number of the dielectric layers, their width, and the porosity percentage. A multilayer structure is constructed using porous silicon material. The porosity level and structural parameters are fine-tuned to achieve the highest attainable sensitivity. Influence of the type and width of the defect layer and the number of dielectric layers, along with the incidence angle, on sensor sensitivity, quality factor and detection limit are analyzed using the transfer matrix method. The sensitivities of the graded and non-graded structures are compared. The linearly graded geometry provides an average sensitivity of 786 nm/RIU with the average detection limit of 7.21×10^{-3} . Furthermore, the paper assesses different sensing parameters such as sensor resolution, detection limit, and signal-to-noise ratio, making the studied structure advantageous for sensor application.

Keywords: linear width grading, photonic crystal, sensors, sensitivity.

<https://doi.org/10.15407/spqeo28.02.239>
PACS 42.79.Pw, 42.79.Qx, 87.85.fk

Manuscript received 24.10.24; revised version received 11.02.25; accepted for publication 11.06.25; published online 26.06.25.

1. Introduction

This article introduces an innovative bio-photonic sensor composed of a porous material, featuring width grading within a photonic structure. This approach is aimed at enhancing the overall sensor performance.

The conception of graded photonic crystals [1, 2] within photonic crystal structures is a relatively recent one. Its primary objective is to enhance the capability of controlling and manipulating light propagation and photonic bandgap engineering from various perspectives and for various configurations. Graded photonic crystals have been deliberately engineered with spatial variations of key parameters such as optical index, fill factor and lattice parameters, allowing for their progressive development [3]. The study of graded photonic crystals [4] is fetching due to a broad range of their applications including enhancement of omnidirectional reflectors width, temperature sensing, and control of photonic bandwidth through refractive index modulation. Graded index optics has attracted significant interest of researchers as a means to improve the sensing performance of the sensors

having Thue–Morse (TM) and double-periodic geometry [5, 6]. TM and double-periodic structures are two types of photonic crystal structures used in photonics and optics to control light propagation in materials. The TM sequence is a mathematical sequence that can be used to design a type of one-dimensional photonic crystal structures based on the TM recursion rule. A double-periodic photonic crystal [5], also known as a bilayer photonic crystal, consists of two alternating layers of different dielectric materials.

Utilizing a gradient refractive index distribution offers an additional design flexibility. This approach allows achieving a significantly high refractive index difference within the same material (*i.e.* silicon in the present work), resulting in minimum interface-induced losses. As a result, it offers the ability to scale designs across user-defined wave-length ranges. Furthermore, this approach effectively alters mode dispersion characteristics, which makes it pivotal for design of beam apertures, deflectors, highly efficient bending waveguides, couplers, self-focusing media, artificial optical black holes, and antireflection coatings [7].

In this study, we enhance sensitivity [8, 9] of the proposed sensor by employing porosity to the layers of the structure and a width grading of the layers. Utilization of porous materials [10, 11] facilitates infiltration of analytes. We compare the sensitivity of a one-dimensional multilayer structure without grading with the sensitivity of a structure with width grading. The novelty of the proposed design is its simple fabrication and, hence, lower overall sensor cost.

The reflection spectrum of a structure having the multilayer linearly graded geometry and its band gap are analyzed using the transfer matrix method (TMM). The finite element method (FEM) [12, 13] is employed to confirm the performance of the linearly-graded geometry by examining mode localization and electric-field distribution profile within the cavity.

The proposed structure with width grading demonstrates a 274% higher sensitivity compared to that of the non-graded structure.

The rest of the paper is organized as follows. In Section 2, theoretical modelling of the geometry is presented. Section 3 outlines the results and discussion. The summary of the work is presented in Section 4.

2. Theoretical modelling of geometry

Here, we investigate a one-dimensional graded width photonic crystal structure for potential sensor applications. At the resonant wavelength λ_r , Eq. (1) determines the width of each layer (d_j) in the reflection spectrum, where n_j represents the refractive index of the j^{th} layer:

$$n_j d_j = \frac{\lambda_r}{4}. \quad (1)$$

The graded layer is assumed to be porous to facilitate analyte infiltration. The porosity (P) of each specific layer can be calculated as follows [14]:

$$P = \frac{(n_f^2 - n_{dm}^2)(n_{an}^2 - 2n_{dm}^2)}{(n_f^2 + 2n_{dm}^2)(n_{an}^2 - n_{dm}^2)}, \quad (2)$$

Here, n_f is the refractive index of the porous layer, n_{dm} is the refractive index of the dense layer and n_{an} is the refractive index of air/analytes, respectively. Changes in porosity have an impact on the effective refractive index of the layers influencing both the transmission and reflection spectrum of the proposed sensor. The non-graded geometry is represented as “Glass/(A/B)³/D/(A/B)³/Air” with a defect layer ‘D’ inserted in between as illustrated in Fig. 1a. The structure is symmetrical and composed of alternating layers of Si (silicon) and PSi (porous silicon). The layer A is a Si (0% porosity) layer and the layer B is a PSi (80% porosity) one as shown in Table 1. In this structure, ‘A’ is characterized by the refractive index $n_h = 3.45$ and ‘B’ has the refractive index $n_l = 1.6$. The width of the layer ‘A’ is 112 nm whereas the width of ‘B’ is 258 nm. These widths are denoted as d_h and d_l , respectively. The layer denoted as ‘D’ serves as the cavity layer. Its refractive index is n_d and its width is denoted as d .

Table 1. Effective refractive indices of Si layers with different porosities.

Porosity in percentage	Refractive index of Si
0	3.45
10	3.2248
20	3.0029
30	2.7826
40	2.5619
50	2.3386
60	2.1097
70	1.8712
80	1.6166
90	1.3346

Fig. 1b shows a structure with a double-graded width configuration. Here, the width of the ‘A’ layer linearly increases and the width of ‘B’ linearly decreases. Specifically, a linear graded index parameter $+\Delta$ (2 nm) and $+2\Delta$ (4 nm) was applied to the high-index layer (as shown for the layer ‘A1’), whereas a linear graded index parameter $-\Delta$ (–10 nm) and -2Δ (–20 nm) was applied to the low-index layer (as shown for the layer ‘B1’).

The layers on both sides of the defect layer exhibit mirror symmetry in both the material compositions and layer widths. The refractive index of Si varying with wavelength (λ_r) is represented by Eq. (3):

$$n_{Si} = 1 + \frac{\lambda^2}{0.0938\lambda^2 - 0.00866}. \quad (3)$$

Use of TMM [15] is particularly well-suited for analyzing reflectivity spectra of both multilayer cavity-based structures with linear width grading and those without grading. A transfer matrix corresponding to the j^{th} layer is defined as follows:

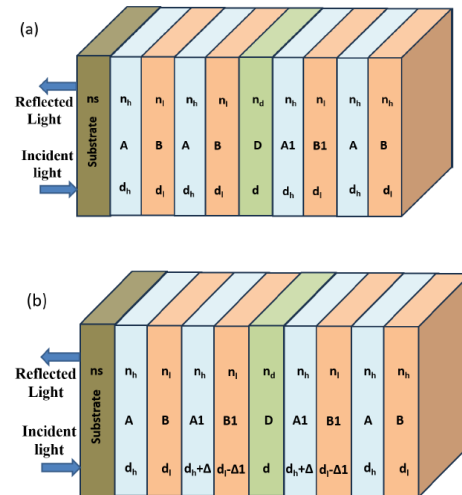


Fig. 1. Geometry without (a) and with (a) width grading.

Table 2. Sensitivities of the structures with the graded and non-graded geometry at 0-degree incidence angle.

Refractive index of analyte	Sensitivity of the structure with the non-graded geometry (nm/RIU)			Sensitivity of the structure with the linearly graded geometry (nm/RIU)		
	$D = d_h$	$D = 2d_h$	$D = 3d_h$	$D = d_h$	$D = 2d_h$	$D = 3d_h$
1.1	50	150	300	210	350	480
1.2	50	165	320	190	375	500
1.3	53.3	170	333.3	196	383.3	493
1.4	57.5	180	340	202.5	397.5	487
1.5	60	188	340	214	398	492

Table 3. Sensitivities of the structures with the graded and non-graded geometry at 20-degree incidence angle.

Refractive index of analyte	Sensitivity of the structure with the non-graded geometry (nm/RIU)			Sensitivity of the structure with the linearly graded geometry (nm/RIU)		
	$D = d_h$	$D = 2d_h$	$D = 3d_h$	$D = d_h$	$D = 2d_h$	$D = 3d_h$
1.1	50	170	340	160	370	570
1.2	60	175	350	190	370	545
1.3	56.6	186	333.3	190	390	576
1.4	62.5	197.5	370	197	397	575
1.5	66	208	382	206	404	568

$$M_j = \begin{bmatrix} \cos \alpha_j & \frac{-j \sin \alpha_j}{p_j} \\ -j p_j \sin \alpha_j & \cos \alpha_j \end{bmatrix}, \quad (4)$$

where $\alpha_j = \frac{2\pi}{\lambda n_j d_j \cos \theta_j}$ and $p_j = n_j \cos \theta_j$ for transverse electric (TE) mode, n_j , d_j and θ_j are the refractive index, width and propagation angle for the j^{th} layer, and the resonating wavelength is λ_r . The resonating wavelength under consideration is 1550 nm. In the context of the suggested multilayer arrangement, the ultimate characteristic matrix is derived by sequentially multiplying the matrices corresponding to each individual layer as follows:

$$M = \prod_{j=1}^N M_j = \begin{bmatrix} M_{11} & M_{12} \\ M_{21} & M_{22} \end{bmatrix}. \quad (5)$$

Here, N represents the count of periods. The reflection coefficient of the suggested multilayer photonic crystal structure is expressed by Eq. (6):

$$r(\omega) = \frac{(M_{11} + M_{12} p_0) p_0 - (M_{21} + M_{22} p_0)}{(M_{11} + M_{12} p_0) - (M_{21} + M_{22} p_0)}. \quad (6)$$

The reflectance of the considered structure can be expressed through the reflection coefficient as follows:

$$R = |r(\omega)|^2. \quad (7)$$

3. Results and discussion

The reflectivity spectrum of the proposed sensor was obtained by simulations using a COMSOL 6.1 software. The sensor performances of the proposed structure with and without linear width grading were compared. Analysis of the geometry functionality involves infiltration of analytes with varying refractive indices into the defect layer. We considered analytes with the refractive indices ranging from 1 to 1.5 with an increment of 0.1. Such analytes are widely applied in biosensors. The resonating wavelength changes when the defect layer is exposed to a substance having the refractive index greater or equal to 1. This change is quantified as the sensor sensitivity.

The sensor sensitivity [16, 17] is calculated by Eq. (8):

$$S = \frac{\Delta \lambda_r}{\Delta n}, \quad (8)$$

where $\Delta \lambda_r$ is the difference of the resonating wavelength at normal refractive index and that at different from normal refractive index and Δn is the difference between the mentioned refractive indices, respectively.

Figs 2a and 2b depict the reflection spectra of the studied structures with two different geometries: the one without grading and the other with linear width grading. The spectra were measured at the width of the cavity layer d_h and zero incidence angle as shown in Table 2. The average sensitivity of the non-graded structure is 54 nm/RIU, whereas the structure with the linearly

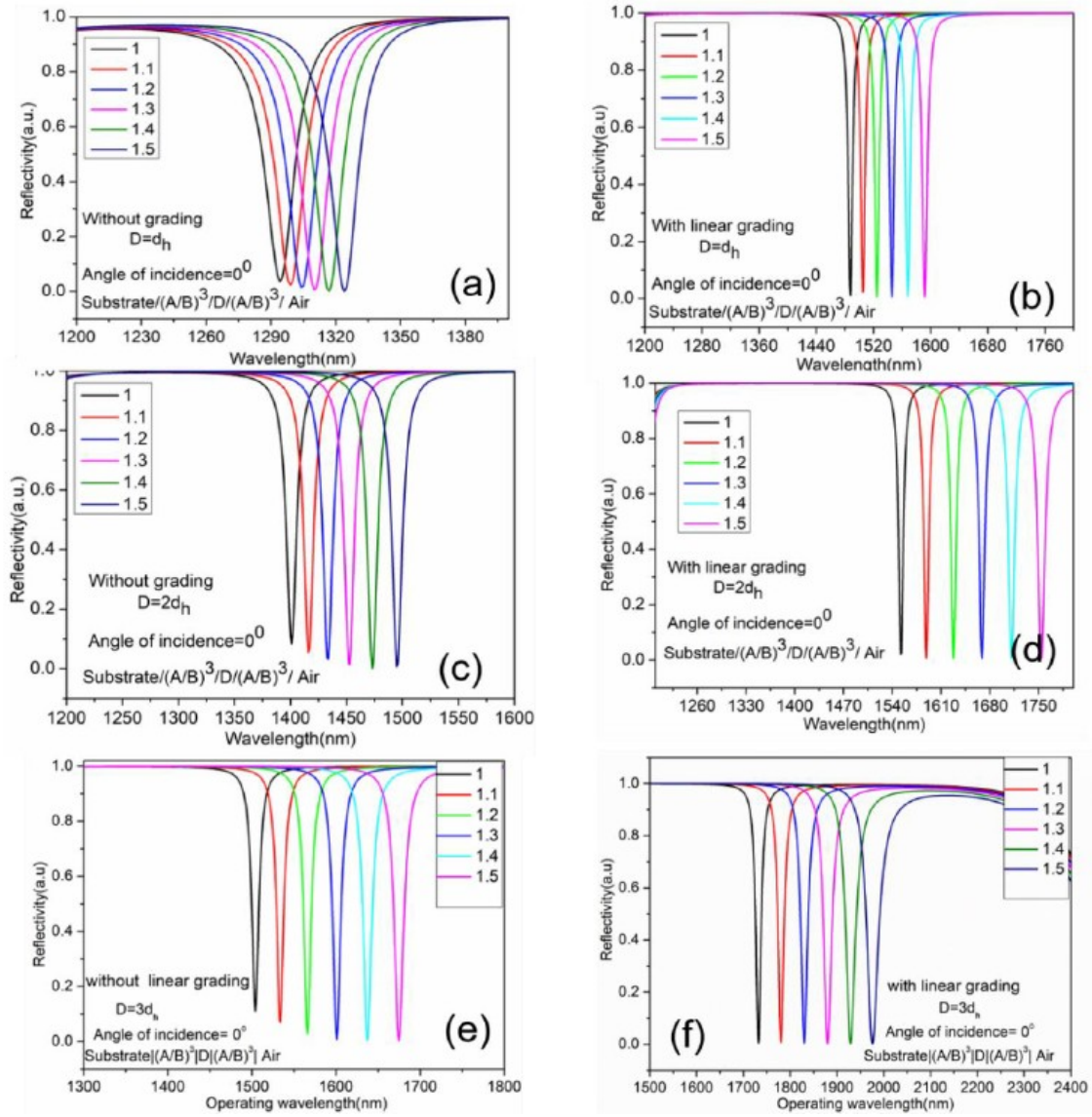


Fig. 2. Reflection spectra of the structures without grading and with linear graded (width grading) geometry with different layer widths, namely d_h , $2d_h$ and $3d_h$, at zero incidence angle.

graded geometry has an average sensitivity of 202 nm/RIU. That is, the linearly graded geometry provides the sensitivity that is 274% higher as compared to that provided by the non-graded geometry. Similarly, in Figs 2c and 2d, one can see the reflection spectra corresponding to two different geometries, namely the one without grading and the other one with linear width grading. These spectra were measured at a zero-incidence angle and the defect layer width $2d_h$ as shown in Table 2. The structures with the non-graded and graded geometries evidence an average sensitivity of 170 and 380 nm/RIU, respectively. It is worth highlighting that the linearly graded geometry provides the sensitivity that is 123% greater as compared to that of the structure with the non-graded geometry.

Fig. 3 shows the reflectivity spectra of the investigated structures with both non-graded and graded

geometries. As indicated in Table 3, the non-graded geometry provides an average sensitivity of 59 nm/RIU, while this value for the case of the graded geometry is 188 nm/RIU being measured at an incidence angle of 20 degrees. The defect layer width is d_h at this. However, when the defect layer width is doubled to $2d_h$, the graded geometry provides an average sensitivity of 386 nm/RIU, surpassing the sensitivity of the structure with the non-graded geometry, which amounts to 187 nm/RIU.

Fig. 4 presents the reflectivity spectra for both the non-graded and graded geometries. According to the data of Table 4, the non-graded geometry provides an average sensitivity of 66 nm/RIU, whereas the graded geometry provides an average sensitivity of 252 nm/RIU at a 40-degree incidence angle and the defect layer width d_h . When the defect layer width is doubled to $2d_h$, the graded geometry demonstrates a substantially higher average

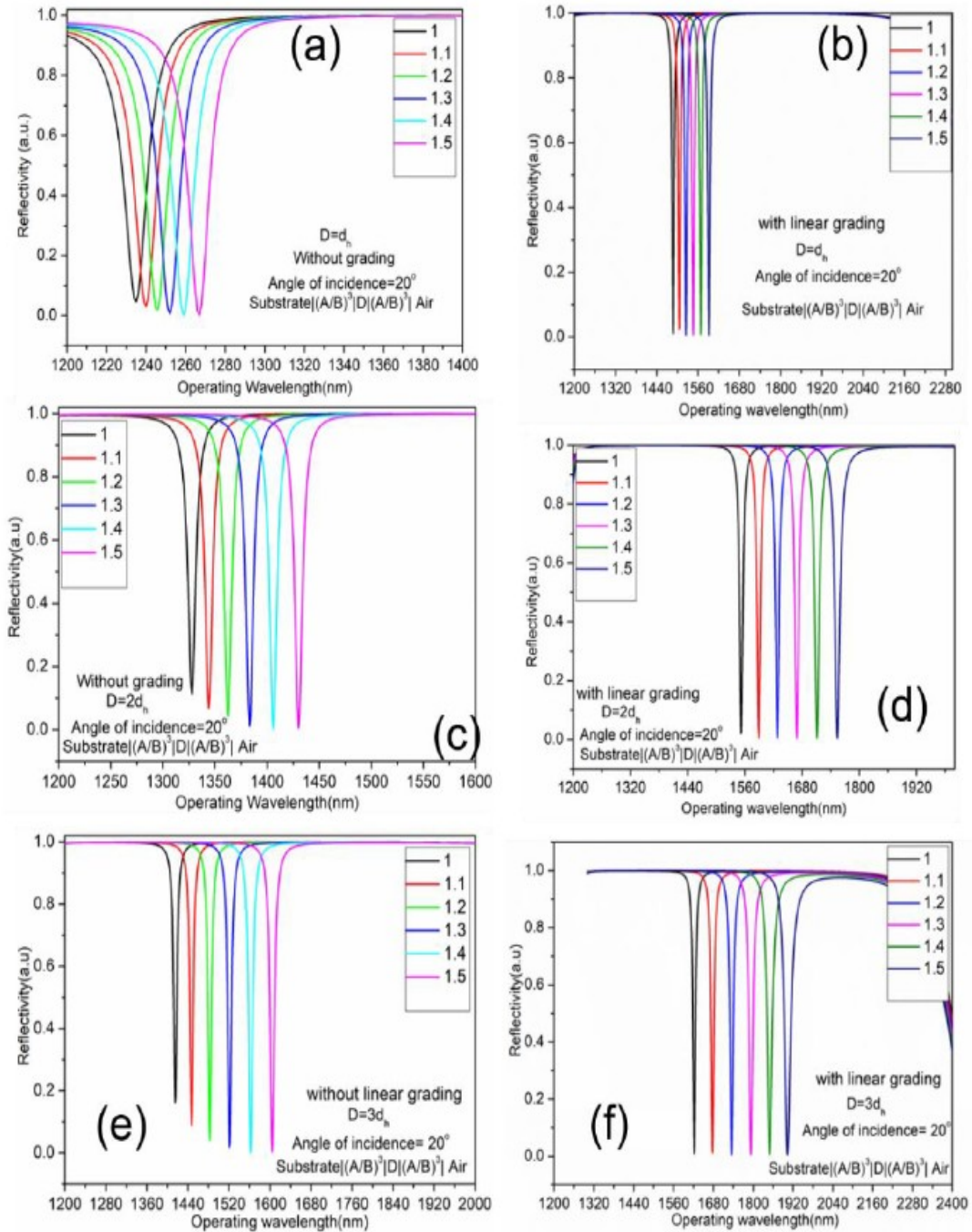


Fig. 3. Reflection spectra of the structures without grading and with linear graded (width grading) geometry with different layer widths, namely d_h , $2d_h$ and $3d_h$, at an incidence angle of 20 degrees.

sensitivity of 505 nm/RIU, surpassing the sensitivity for the non-graded geometry case, which remains at 209 nm/RIU. Fig. 5 shows a comparison of the average sensitivities for the graded and non-graded geometries at different incidence angles. Three scenarios are considered: (a) the defect layer width is d_h , (b) the defect layer width is $2d_h$, and (c) the defect layer width is $3d_h$. Fig. 5d shows a comparison of the electric field intensities for the linearly graded geometry case at various incidence angles at the cavity layer width $3d_h$.

As can be seen from this figure, the electric field intensity values are 5.18×10^5 , 6.61×10^5 , and 1.0×10^6 V/m for the 0-, 20- and 40-degree incidence angles, respectively.

In addition to sensitivity, other sensor performance parameters have been calculated as shown in Table 5. The minimum refractive index (RI) change that can be detected by the sensor is the detection limit (DL) calculated by dividing the sensor resolution to its sensitivity, $DL = SR/S$ [18].

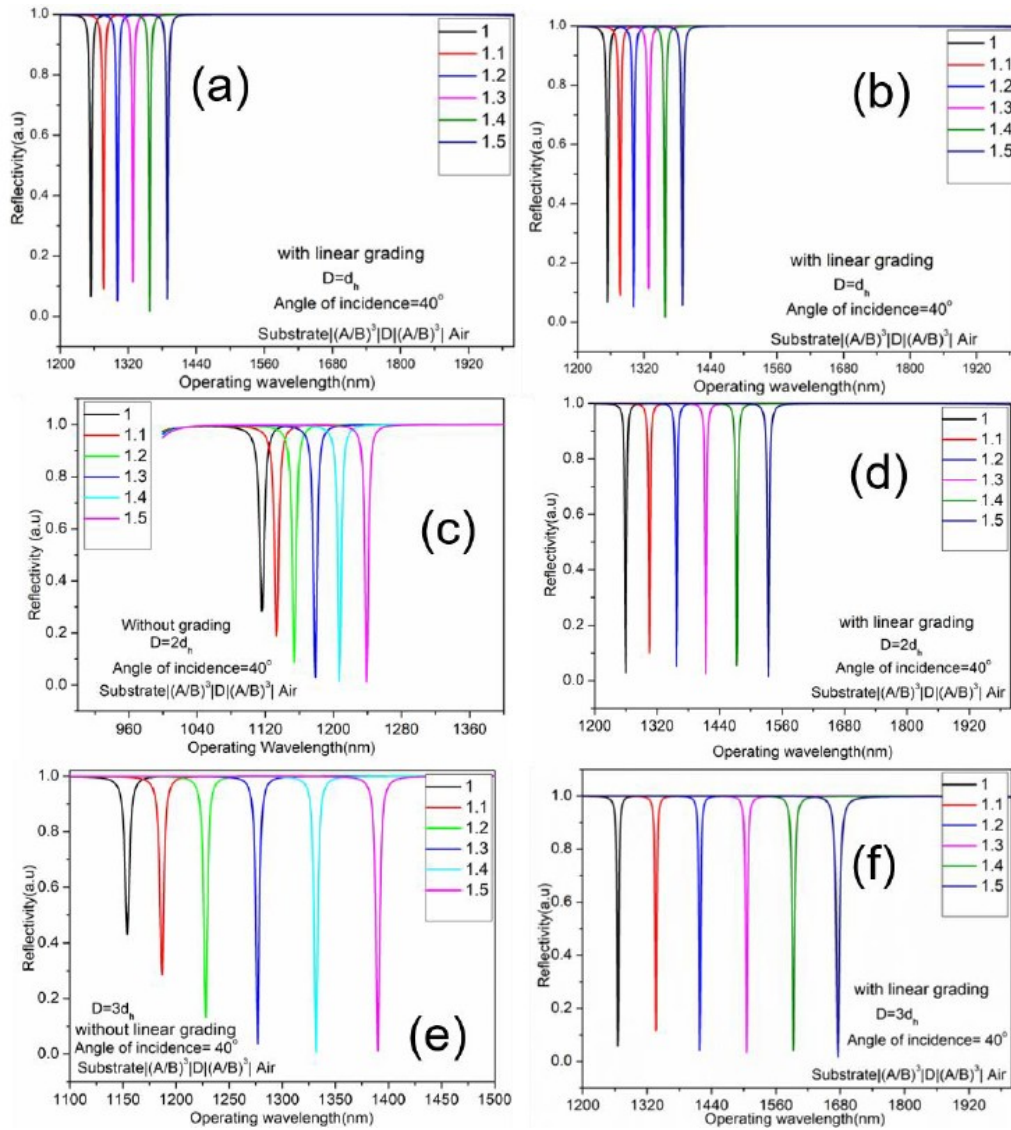


Fig. 4. Reflection spectra of the structures without grading and with linear graded (width grading) geometry with different layer widths, namely d_h , $2d_h$ and $3d_h$, at an incidence angle of 40° .

Table 4. Sensitivities of the structures with the graded and non-graded geometry at 40° -degree incidence angle.

Refractive index of analyte	Sensitivity of the structure with the non-graded geometry (nm/RIU)			Sensitivity of the structure with the linearly graded geometry (nm/RIU)		
	$D = d_h$	$D = 2d_h$	$D = 3d_h$	$D = d_h$	$D = 2d_h$	$D = 3d_h$
1.1	60	170	320	240	450	710
1.2	60	190	365	240	485	765
1.3	66.6	216	413.3	250	516	803
1.4	70	227.5	447.5	262	532	827
1.5	76	246	472	270	546	826

The sensor resolution (SR) [19] refers to the minimum spectral shift that can be detected, $SR = FWHM / ((1.5) \times (SNR)^{0.25})$, where FWHM is the full width at half maximum and SNR is the signal-to-

noise ratio, respectively. The quality factor (QF) [20] is defined as $QF = \lambda_r / FWHM$, where λ_r is the resonant wavelength. The figure of merit (FOM) is calculated as $FOM = S / FWHM$ [21].

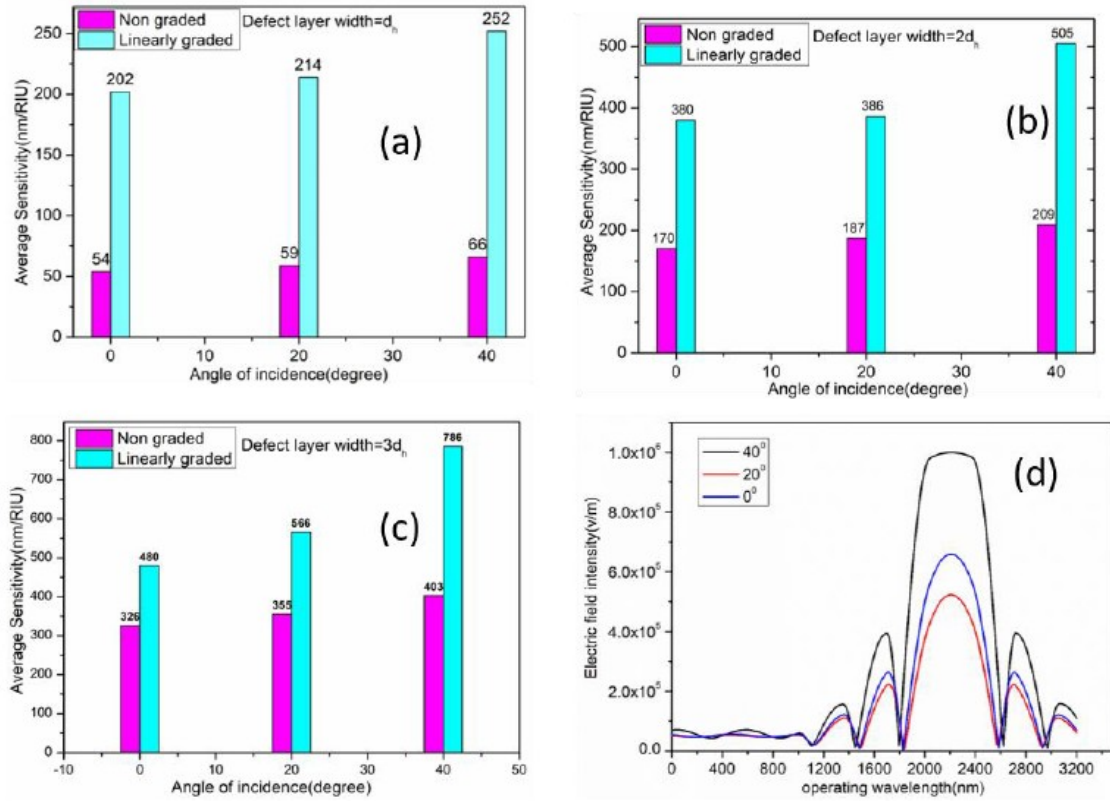


Fig. 5. Average sensitivity for the graded and non-graded geometry cases at various incidence angles and the cavity layer width d_h (a), $2d_h$ (b), and $3d_h$ (c). (d) Electric field intensity for the structures with the linear graded geometry at various incidence angles and the cavity layer width $3d_h$.

Table 5. The proposed linear width grading sensor sensitivity, signal-to-noise ratio, detection limit, and sensor resolution for different infiltrated analytes, at an incidence angle of 40-degree and the defect layer width $3d_h$.

Refractive index of analyte	S (nm/RIU)	SNR	Detection limit	Sensor resolution
1.1	710	78	0.00627851	4.457742
1.2	765	155	0.00691851	5.292662
1.3	803	240	0.00735239	5.903969
1.4	827	296	0.00752331	6.221773
1.5	826	378	0.00800726	6.614

It may be concluded therefore that by altering the incidence angle and increasing the cavity width, the sensitivity of the structure can be enhanced, ultimately boosting its overall performance. The proposed bio-photonic sensor, employing a graded index, exhibits a higher sensitivity as compared to that of the sensors with a conventional step index profile. Incorporating a graded refractive index profile has an additional benefit of reducing the interface-related losses within the stacked photonic crystal structure. Furthermore, introduction of the width graded index enables controlling the mode confinement characteristics of the structure, resulting in a pronounced increase in electric field confinement

($>1 \times 10^6$ V/m) within the defect region. This enhanced confinement increases the interaction between light and matter, thereby raising the sensitivity.

In conclusion, Table 5 enables making a comparative analysis between the obtained outcomes and previous endeavors by the optics research community. The sensitivity of the envisioned structure can be readily adjusted by manipulating the incidence angle without a need to fulfil phase-matching conditions akin those encountered in structures based on surface plasmon resonance. The fabrication process of the structures with the suggested design will be simplified by employing presently available thin film deposition methods.

4. Summary

The current study explores a width graded photonic crystal cavity geometry denoted as Substrate/(AB)³/D/(AB)³/Air for potential photonic sensing applications. The graded width geometry provides a 274% greater sensitivity as compared to that of the structures with the non-graded photonic crystal geometry. Further enhancements in sensitivity can be achieved by adjusting specific sensor parameters such as the incidence angle and cavity layer width. Furthermore, by triplicating the width of the defect layer in the suggested graded width design, the average sensitivity can be increased to 786 nm/RIU at an incidence angle of 40 degrees. The achieved sensitivity is high enough to enable detecting extremely low concentrations of analytes. Moreover, the simplicity and cost-effectiveness of the fabrication process make the proposed structure a promising choice for various sensing applications, including gas sensing, liquid sensing, and detection of various biological components.

References

- Centeno E., Cassagne D. Graded photonic crystals. *Opt. Lett.* 2005. **30**, Issue 17. P. 2278–2280. <https://doi.org/10.1364/OL.30.002278>.
- Centeno, E., Cassagne D., Albert J.-P. Mirage and superbending effect in two-dimensional graded photonic crystals. *Phys. Rev. B.* 2006. **73**, Issue 23. P. 235119. <https://doi.org/10.1103/PhysRevB.73.235119>.
- Fan C.Z., Wang, J.Q., He J.N. *et al.* Theoretical study on the photonic band gap in one-dimensional photonic crystals with graded multilayer structure. *Chin. Phys. B.* 2013. **22**, Issue 7. <https://doi.org/10.1088/1674-1056/22/7/074211>.
- Dash D., Saini J. Linearly graded photonic crystal with improved sensitivity for sensing application. *2022 8th Int. Conf. on Signal Processing and Communication (ICSC)*, Noida, India, 2022. P. 144–146. <https://doi.org/10.1109/ICSC56524.2022.10009517>.
- Singh, B.K., Pandey P.C. Influence of graded index materials on the photonic localization in one-dimensional quasiperiodic (Thue–Mosre and Double-Periodic) photonic crystals. *Opt. Commun.* 2014. **333**. P. 84–91. <https://doi.org/10.1016/j.optcom.2014.07.043>.
- Goyal A.K., Massoud Y. Interface edge mode confinement in dielectric-based quasi-periodic photonic crystal structure. *Photonics.* 2022. **9**, Issue 10. P. 676. <https://doi.org/10.3390/photonics9100676>.
- Kumar R., Srivastava S.K., Srivastava S.K. A comparative study of transmission mode tunability in, linearly graded and without graded, defect photonic crystal structure. *J. Nanoeng. Nanomanuf.* 2017. **6**, Issue 3. P. 1–11. <https://doi.org/10.1166/jnan.2016.1280>.
- Mohapatra B., Khan A.S., Dash D. *et al.* Design of biosensor using 1D photonic crystal for dengue virus detection. *2022 4th Int. Conf. on Advances in Computing, Communication Control and Networking (ICAC3N)*, 2022. <https://doi.org/10.1109/ICAC3N56670.2022.10074441>.
- Hao J.-J., Gu K.-D., Xia L. *et al.* Research on low-temperature blood tissues detection biosensor based on one-dimensional superconducting photonic crystal. *Commun. Nonlinear Sci. Numer. Simul.* 2020. **89**. P. 105299. <https://doi.org/10.1016/j.cnsns.2020.105299>.
- Goyal A.K., Dutta H.S., Pal S. Porous photonic crystal structure for sensing applications. *J. Nanophotonics.* 2018. **12**, Issue 4. P. 040501. <https://doi.org/10.1117/1.jnp.12.040501>.
- Goyal A.K., Dutta H.S., Pal S. Development of uniform porous one-dimensional photonic crystal based sensor. *Optik (Stuttg.)*. 2020. **223**. P. 165597. <https://doi.org/10.1016/j.ijleo.2020.165597>.
- Bao G., Li P. Finite Element Methods. In: *Applied Mathematical Sciences (Switzerland)*. 2022. **208**. P. 87–161. https://doi.org/10.1007/978-981-16-0061-6_4.
- Jin J.-M. *The Finite Element Method in Electromagnetics*, 3rd Edition. Wiley-IEEE Press, 2014.
- Canham L. (Ed.) *Handbook of Porous Silicon*. 2nd Edition. Springer, 2018.
- Lin L.L., Li Z.Y., Ho K.M. Lattice symmetry applied in transfer-matrix methods for photonic crystals. *J. Appl. Phys.* 2003. **94**, Issue 02. <https://doi.org/10.1063/1.1587011>.
- Goyal A.K., Dash D., Saini J., Massoud Y. Theoretical analysis of graded-index topological resonator for improved sensing performance. *Opt. Express.* 2024. **32**, Issue 03. <https://doi.org/10.1364/oe.511412>.
- Dash D., Saini J. Sensitivity analysis of step index and graded index one dimensional cavity-based cholesterol sensor. *Opt. Quantum Electron.* 2023. **55**, No 04. <https://doi.org/10.1007/s11082-023-04587-1>.
- Saurav K., Le Thomas N. Probing the fundamental detection limit of photonic crystal cavities: Erratum. *Optica.* 2017. **4**, Issue 10. <https://doi.org/10.1364/optica.4.001305>.
- Tsai T., Wang C., Wang H. *et al.* A high-resolution refractive index sensor based on a magnetic photonic crystal. *Int. J. Phys. Math. Sci.* 2015. **9**, Issue 07.
- Deotare P.B., McCutcheon M.W., Frank I.W. *et al.* High quality factor photonic crystal nanobeam cavities. *Appl. Phys. Lett.* 2009. **94**, Issue 12. P. 121106. <https://doi.org/10.1063/1.3107263>.
- Bijalwan A., Rastogi V. Gold–aluminum-based surface plasmon resonance sensor with a high-quality factor and figure of merit for the detection of hemoglobin. *Appl. Opt.* 2018. **57**, Issue 31. P. 9230–9237. <https://doi.org/10.1364/ao.57.009230>.
- Saini S.K., Awasthi S.K. Sensing and detection capabilities of one-dimensional defective photonic crystal suitable for malaria infection diagnosis from preliminary to advanced stage: Theoretical study.

Crystals (Basel). 2023. **13**, Issue 01. P. 128. <https://doi.org/10.3390/cryst13010128>.

23. Segovia-Chaves F., Trujillo J.C., Trabelsi Y. Enhanced the sensitivity of one-dimensional photonic crystals infiltrated with cancer cells. *Mater. Res. Express*. 2023. **10**, Issue 02. P. 026202. <https://doi.org/10.1088/2053-1591/acb907>.
24. Sampath D., Narasimhan V. One-dimensional defect layer photonic crystal sensor for purity assessment of organic solvents. *ACS Omega*. 2024. **9**, Issue 08. P. 9625–9632. <https://doi.org/10.1021/acsomega.3c09589>.
25. Birhanu R., Gemta A.B., Tolessa Maremi F., Kumela A.G. One-dimensional photonic crystal biosensors encompassing defect layer for blood-stream bacteria detection. *J. Opt.* 2024. **53**. P. 4853–4864. <https://doi.org/10.1007/s12596-024-01665-9>.

Authors and CV



Baibaswata Mohapatra, Ph.D., Professor & Dean-R&D at the Greater Noida Institute of Technology (Eng. Institute), Greater Noida, UP, India. Dr. Mohapatra has about 24 years of teaching and research experience. He has supervised 4 doctoral students and 15 M.Tech students in Commu-

nication and Networking. He has more than 50 publications and 10 Indian patents. He is also associated with various professional societies at international and national level during more than 15 years. Some of these include: Member of IEEE, USA, Life Member of IETE (Institute of Electronics and Telecommunication) India, Life Member of ISTE (Indian Society for Technical Education) India, and Life Member of OBA (Odisha Bigyan Academy), Bhubaneswar.



Diptimayee Dash, defended her Ph.D. thesis in Photonics in 2024 at the Jaypee Institute of Information & Technology, Noida, India. Associate Professor at the EEE department of the Galgotias College of Engineering & Technology, Greater Noida, India.

She authored many journal and conference papers in the area of photonics. The area of her scientific interests includes electromagnetics, and biosensors using photonic crystals. E-mail: dash.diptimayee@gmail.com, <https://orcid.org/0000-0001-7564-8029>



Dhiraj Gupta has received the M.Tech and Ph.D. degrees from the MNNIT, Allahabad and JMI University, New Delhi. He is working as the Director of the Greater Noida Institute of Technology (Eng. Institute), Greater Noida since 2021.

He has more than 25 years of teaching, research and administrative experience. He has guided many PG and Ph.D. students and published more than 30 research articles in international journals and conference proceedings. He is a member of professional societies, such as IEEE, USA, and ISTE, New Delhi.

Authors' contributions

Mohapatra B.: formal analysis, investigation, data curation (partially), writing – original draft, writing – review & editing, visualization.

Dash D.: conceptualization, methodology, validation, formal analysis, investigation, resources, data curation, writing – original draft, writing – review & editing.

Gupta D.: review & editing, validation, investigation.

Покращення чутливості датчика та взаємодії світла з речовиною завдяки лінійному градуванню ширини

B. Mohapatra, D. Dash, D. Gupta

Анотація. У цій статті запропоновано фотонний кристал з лінійним градуванням товщини, який має розташований по центру дефектний шар, спеціально розроблений для застосування у датчиках. Конструкція включає чергування шарів діелектричного матеріалу на скляній підкладці. Цілеспрямоване створення пористої структури в кожному шарі полегшує проникнення аналіту та підвищує чутливість. Проведено комплексний аналіз з метою оптимізації кількості шарів діелектрика, їхньої товщини та пористості. Багатошарова структура побудована з використанням пористого кремнію. Рівень пористості та структурні параметри підібрані так, щоб досягти найвищої можливої чутливості. Вплив типу та товщини дефектного шару, а також кількості шарів діелектрика та кута падіння на чутливість датчика, добротність та поріг виявлення було проаналізовано з використанням методу матриць переходу. Порівняно чутливості градуйованих та неградуйованих структур. Середня чутливість датчиків, що мають геометрію з лінійним градуванням, становить 786 нм/RIU, а середнє значення порогу виявлення – $7,21 \times 10^{-3}$. У статті також оцінено різні параметри детектування, такі як роздільна здатність датчика, поріг виявлення та співвідношення сигнал/шум, які надають переваг для застосувань у датчиках.

Ключові слова: лінійна градація ширини, фотонний кристал, датчики, чутливість.